



HAL
open science

AC electrical architecture propelling systems for aeronautics

Alexandre Richard, Florent Rougier, Xavier Roboam, Nicolas Roux, Hubert
Piquet

► **To cite this version:**

Alexandre Richard, Florent Rougier, Xavier Roboam, Nicolas Roux, Hubert Piquet. AC electrical architecture propelling systems for aeronautics. MEA 2021 More Electric Aircraft, SEE - 3AF, Oct 2021, Bordeaux, France. hal-03419609v2

HAL Id: hal-03419609

<https://hal.science/hal-03419609v2>

Submitted on 16 Nov 2021

HAL is a multi-disciplinary open access archive for the deposit and dissemination of scientific research documents, whether they are published or not. The documents may come from teaching and research institutions in France or abroad, or from public or private research centers.

L'archive ouverte pluridisciplinaire **HAL**, est destinée au dépôt et à la diffusion de documents scientifiques de niveau recherche, publiés ou non, émanant des établissements d'enseignement et de recherche français ou étrangers, des laboratoires publics ou privés.

AC electrical architecture propelling systems for aeronautics

A. RICHARD (1,2), F. ROUGIER (1), X. ROBOAM (2), N. ROUX (2), H. PIQUET (2)

1 : Safran TECH Toulouse, 1 rue Louis Blériot 31702 Blagnac Cedex, France –
alexandre.richard@safrangroup.com - florent.rougier@safrangroup.com

2 : LAPLACE Université de Toulouse, CNRS, INPT, UPS, Toulouse, France, xavier.roboam - nicolas.roux –
hubert.piquet - @laplace.univ-tlse.fr

Abstract

This paper describes the study of an original (“power electronic-less”) AC electrical architecture for propulsive purposes in aeronautics. This architecture is composed of two or more Permanent Magnets Synchronous Machines (PMSM) directly linked to each other by an AC bus, one in generator mode driven by a gas turbine and all the other PMSM in motor mode, each one driving a propeller. The simple architecture with only two PMSM – one generator and one motor – will be mainly developed here. Although this architecture may seem too rigid to be implemented, the absence of power electronic offers potential savings in mass and costs, which justifies its study to determine whether this architecture could be implemented and used for propelling systems or not. This paper focuses on the development of an analytical model enabling to fully describe the dynamic and permanent behaviour of such an architecture. Once this model is set, the stability of the architecture is analysed: a classical approach, with the linearization of the analytical model and the use of root locus analysis, is considered.

Introduction

With the evolution of aircraft propulsion towards greener solutions, fully electrical configurations are more and more studied. Most architectures are proposed around a DC bus with or without hybridization with auxiliary electric sources (batteries or fuel cells) [1]. They need AC/DC and DC/AC converters to interface AC electric generators and motors. This paper proposes a “power electronic-less” architecture that directly links through an AC bus two PMSM or more, one in generator mode driven by a gas turbine and the other one(s) in motor mode driving one (or several) propeller(s).

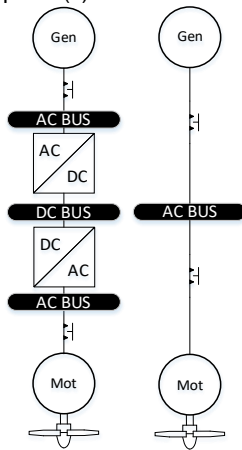


Figure 1 : DC (left) – AC (right) architectures for a single propeller channel

This would enable suppressing power electronics thus making potential savings in mass and costs. However, this AC architecture may be too “rigid” to be implemented; indeed removing power electronics blocks creates a constraint between the speeds of the two PMSM, which raises questions on the stability and the dynamic behaviour of this architecture.

Development of the analytical model

In order to be as close as possible to the simple (single channel) application case considered here, the studied system is composed of the electrical architecture previously described to which is added a representation of a speed controlled gas turbine. This addition is done to take in to account the gas turbine that is linked to the system and the influence it could have on it. An IP controller thus represents the gas turbine, as this structure enable to depict the behaviour of a gas turbine from the point of view of the electrical architecture. As presented in **Figure 2** this system has therefore two inputs:

- The speed set point as a gas turbine input (ω_{gref})
- The load torque set point as a propeller input (Γ_{ch})

And six state variables:

- The two components of the currents of the AC bus (expressed in a Park’s reference frame: I_d, I_q), both common for generator and motor
- The speeds of the generator and of the motor (ω_g, ω_m)
- The load torque of the gas turbine (GT) (T_{TAG})
- The difference between rotor positions of generator and motor named the rotor angle (δ)

The objective is to obtain a state model representation in the following form:

$$\frac{d}{dt} \begin{pmatrix} I_d \\ I_q \\ \delta \\ \omega_m \\ \omega_g \\ T_{TAG} \end{pmatrix} = A \begin{pmatrix} I_d \\ I_q \\ \delta \\ \omega_m \\ \omega_g \\ T_{TAG} \end{pmatrix} + B \begin{pmatrix} \omega_{gref} \\ \Gamma_{ch} \end{pmatrix} \quad (1)$$

The document will now focus on the electrical part of the system that can be seen in **Figure 3**. This approach has as starting point the Behn-Eschenburg model of the electric architecture, putting end-to-end the Behn-Eschenburg models of the two PMSM.

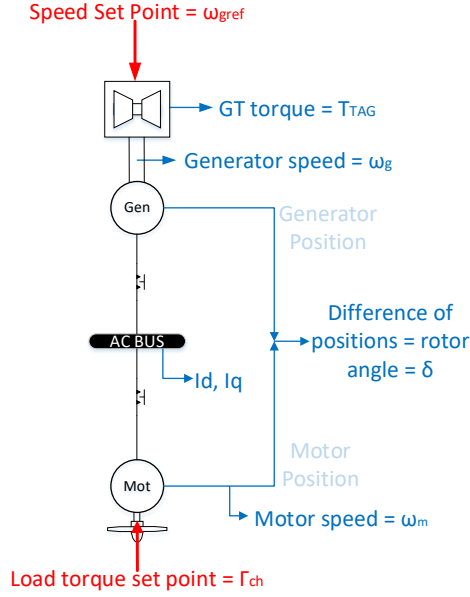


Figure 2 : Considered system

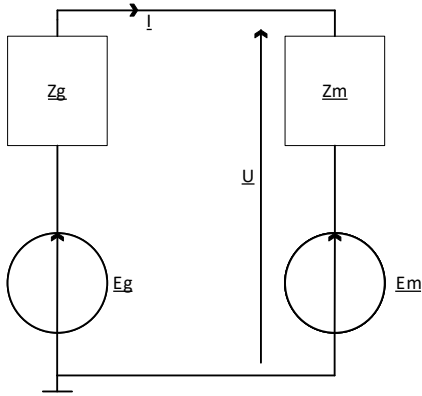


Figure 3 : Electrical component of the system

In order to establish the model, the two PMSM are firstly considered separately in their particular reference frame and at first, their ABC reference frame (generator equations (2) and motor equations (3)):

$$U_{abc} = -R_g I_{abc} + \frac{d}{dt} \Phi_{g_{abc}}; \Phi_{g_{abc}} = -L_g I_{abc} + \phi_{a_g} \quad (2)$$

$$U_{abc} = R_m I_{abc} + \frac{d}{dt} \Phi_{m_{abc}}; \Phi_{m_{abc}} = L_m I_{abc} + \phi_{a_m} \quad (3)$$

With $\phi_{a_i} = \phi_{a_i} \begin{pmatrix} \cos(\theta_i) \\ \cos(\theta_i - \frac{2\pi}{3}) \\ \cos(\theta_i - \frac{4\pi}{3}) \end{pmatrix}$ the permanent magnet

flux, $R_i = \begin{pmatrix} R_i & 0 & 0 \\ 0 & R_i & 0 \\ 0 & 0 & R_i \end{pmatrix}$, $L_i = \begin{pmatrix} L_{i_{aa}} & M_{i_{ab}} & M_{i_{ac}} \\ M_{i_{ba}} & L_{i_{bb}} & M_{i_{bc}} \\ M_{i_{ca}} & M_{i_{cb}} & L_{i_{cc}} \end{pmatrix}$ and

$\theta_i = \omega_i t$ with ω_i the pulsation.

The system is then described thanks to alternative values. It is therefore necessary to carry changes of reference frame with a Park's transformation in order to describe the system with continuous quantities in the reference frame DQ0. After using the Park's transformation the equations describing the generator ((4) & (5)) and the motor ((6) & (7)) are expressed in the particular reference frame DQ0 of each PMSM ('g' for

generator and 'm' for the motor) :

$$U_{dq0}^g = -R_g I_{dq0}^g + \frac{d}{dt} (\Phi_{g_{dq0}}^g) + \omega_g \begin{pmatrix} 0 & -1 & 0 \\ 1 & 0 & 0 \\ 0 & 0 & 0 \end{pmatrix} \Phi_{g_{dq0}}^g \quad (4)$$

$$\Phi_{g_{dq0}}^g = -L_g I_{dq0}^g + \phi_{a_g} \begin{pmatrix} 1 \\ 0 \\ 0 \end{pmatrix} \quad (5)$$

$$U_{dq0}^m = R_m I_{dq0}^m + \frac{d}{dt} (\Phi_{m_{dq0}}^m) + \omega_m \begin{pmatrix} 0 & -1 & 0 \\ 1 & 0 & 0 \\ 0 & 0 & 0 \end{pmatrix} \Phi_{m_{dq0}}^m \quad (6)$$

$$\Phi_{m_{dq0}}^m = L_m I_{dq0}^m + \phi_{a_m} \begin{pmatrix} 1 \\ 0 \\ 0 \end{pmatrix} \quad (7)$$

Until this point, the two PMSM are described separately in their particular DQ0 reference frames. Consequently, the two equations can not be linked at this point and in order to describe the whole system, the same DQ0 reference frame must be used to couple both machine electrical equations. The DQ0 reference frame of the generator is chosen to be this common DQ0 reference frame as it can be used in a similar way in the case where there would be several motors, it also enables to describe easily the position of motor compared to the generator with only the variable δ . This means that the equations of the motor have to undergo a transformation from the DQ0 reference frame of the motor to the DQ0 reference frame of the generator. Finally, after simplifications, the equations of the generator and the motor in the DQ0 reference frame of the generator can be expressed as follows:

$$U_{dq0}^g = -R_g I_{dq0}^g - L_g \frac{d}{dt} (I_{dq0}^g) - L_g \omega_g \begin{pmatrix} 0 & -1 & 0 \\ 1 & 0 & 0 \\ 0 & 0 & 0 \end{pmatrix} I_{dq0}^g + \omega_g \phi_{a_g} \begin{pmatrix} 1 \\ 1 \\ 0 \end{pmatrix} \quad (\text{generator}) \quad (8)$$

$$U_{dq0}^g = R_m I_{dq0}^g + L_m \frac{d}{dt} (I_{dq0}^g) + L_m \omega_g \begin{pmatrix} 0 & -1 & 0 \\ 1 & 0 & 0 \\ 0 & 0 & 0 \end{pmatrix} I_{dq0}^g + \omega_m \phi_{a_m} \begin{pmatrix} \sin(\delta) \\ \cos(\delta) \\ 0 \end{pmatrix} \quad (\text{motor}) \quad (9)$$

The two systems of equations being in the same DQ0 reference frame, it is possible to couple them finally obtaining:

$$(L_g + L_m) \frac{d}{dt} (I_{dq0}^g) = -(R_g + R_m) I_{dq0}^g - (L_g + L_m) \omega_g \begin{pmatrix} 0 & -1 & 0 \\ 1 & 0 & 0 \\ 0 & 0 & 0 \end{pmatrix} I_{dq0}^g - \omega_m \phi_{a_m} \begin{pmatrix} \sin(\delta) \\ \cos(\delta) \\ 0 \end{pmatrix} + \phi_{a_g} \omega_g \begin{pmatrix} 1 \\ 1 \\ 0 \end{pmatrix} \quad (10)$$

To this electrical part of the state model, mechanical equations have to be added in order to fully describe the system:

$$\frac{d}{dt} \delta = \frac{d}{dt} (\theta_g - \theta_m) = \omega_g - \omega_m \quad (11)$$

$$J_m \frac{d}{dt} \omega_m = p_m (T_{em_m} - \Gamma_{ch}) \quad (12)$$

With $T_{em_m} = \frac{3p_m}{2\omega_m} \text{Re}(V_{dq0}^g I_{dq0}^{g*})$ knowing that:

$$V_{dq0}^g = L_m \frac{d}{dt} \begin{pmatrix} I_d^g \\ I_q^g \\ 0 \end{pmatrix} + L_m \omega_g \begin{pmatrix} 0 & -1 & 0 \\ 1 & 0 & 0 \\ 0 & 0 & 0 \end{pmatrix} I_{dq0}^g + \omega_m \phi_{a_m} \begin{pmatrix} \sin(\delta) \\ \cos(\delta) \\ 0 \end{pmatrix} \quad (13)$$

This result in having:

$$T_{em_m} = \frac{3p_m}{2} \Phi_{a_m} \left(1 - \frac{L_m}{L_g + L_m} \right) (I_d \sin(\delta) + I_q \cos(\delta)) - \frac{3p_1 L_m}{2\omega_m} \left(\frac{R_g + R_m}{L_g + L_m} (I_d^2 + I_q^2) + \frac{\Phi_{a_g}}{L_g + L_m} \omega_g I_q \right) \quad (14)$$

In the same way, the equations from the controller standing for the gas turbine have to be added (the case of an IP controller is presented here) according to the following scheme :

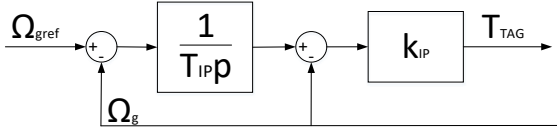


Figure 4 Speed controller representing the GT

$$\frac{d\omega_g}{dt} = \frac{p_g}{J_{eq_g}} (T_{TAG} - T_{em_g}) \quad \text{avec } J_{eq_g} = J_g + J_{TAG} \quad (15)$$

$$\frac{dT_{TAG}}{dt} = \frac{k_{IP}}{T_{IP}} * \frac{\omega_{gref}}{p_g} - \frac{k_{IP}}{T_{IP}} * \frac{\omega_g}{p_g} - \frac{k_{IP}}{p_g} * \frac{d\omega_g}{dt} \quad (16)$$

With $T_{em_g} = \frac{3p_g}{2\omega_g} \text{Re}(V_{dq0}^g I_{dq0}^{g*})$ and

$$V_{dq0}^g = -L_g \frac{d}{dt} \begin{pmatrix} I_d^g \\ I_q^g \\ 0 \end{pmatrix} - L_g \omega_g \begin{pmatrix} 0 & -1 & 0 \\ 1 & 0 & 0 \\ 0 & 0 & 0 \end{pmatrix} I_{dq0}^g + \omega_g \phi_{a_g} \begin{pmatrix} 0 \\ 1 \\ 0 \end{pmatrix} \quad (17)$$

This result in having:

$$T_{em_g} = \frac{3p_g}{2} \Phi_{a_g} \left(1 - \frac{L_g}{L_g + L_m} \right) I_q + \frac{3p_g L_g}{2\omega_g} \left(\frac{R_g + R_m}{L_g + L_m} (I_d^2 + I_q^2) + \frac{\Phi_{a_m} \omega_1}{L_g + L_m} (I_d \sin(\delta) + I_q \cos(\delta)) \right) \quad (18)$$

Thanks to all these equations, the state model (1) is complete and can describe the performances of the AC architecture.

Stability Study: linearized approach with root locus

After establishing the analytical model, the main idea is to study the stability of the AC architecture thanks to the analytical model using the root-locus analysis to characterize possible oscillations or stall situations. The objective of this approach is to find a stability criterion or at least to clarify the conditions of use that would enable a system operation without any instability.

As it can be seen in the development above, the state model is non-linear and needs first to be "small signal linearized" before using the root locus approach.

Once the system is linearized around a steady state point, the root-locus can be displayed as on the **Figure 5**. On the **Figure 5**, six poles are visible as the state

model is a six order model.

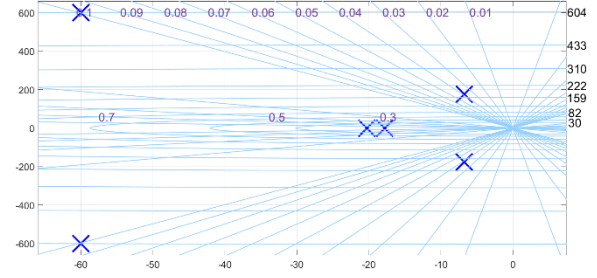


Figure 5 : Root locus display

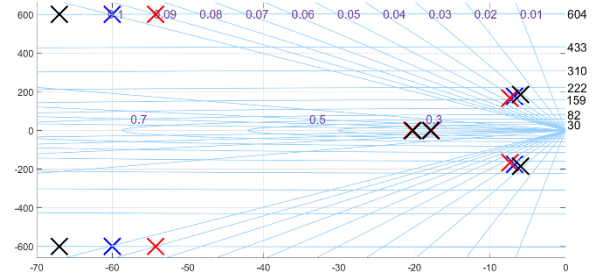


Figure 6 : Example of variation of parameters (variation of inductances values (red increase – black decrease of inductances values))

After sensibility studies done by varying main parameters (electrical, mechanical and input parameters) it is possible to identify the origins of each pole expressed from the state model.

In the example of **Figure 6**, a variation of inductances values is done; one pair of poles varies with a high intensity compared to the others. This indicates that this pair of poles is linked to the electrical equations describing the evolution of currents, seen previously.

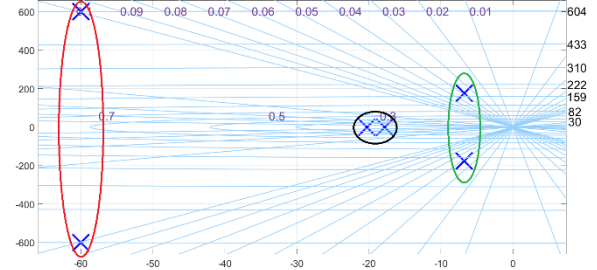


Figure 7 : Association of the poles with the physical field (red : electrical, green : mechanical, black : control of the gas turbine)

From parameter sensitivity analysis, it is possible to associate the different pole pairs to the different domains – electrical, mechanical, control of the gas turbine. The results are presented in **Figure 7**.

Due to its position and its evolution according to parametric variations, the pole pairs that can create oscillations and potentially instabilities are the ones associated to the mechanical domain (in green on the previous figure). For instance, the previous figures were established given a particular steady state point. The idea is now to study the evolution of the poles with respect to the system operation at steady state and to compare this evolution to a transient time simulation of the system crossing the corresponding steady states. The evolution of the pole pair related to the mechanical

mode is displayed below for a range of steady states:

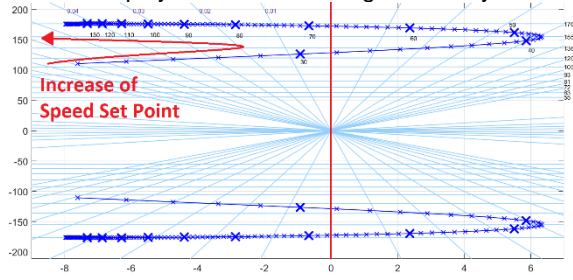


Figure 8 : Example of evolution of the root locus (pole pair related to mechanical domain) for several steady states (motor mechanical speed)

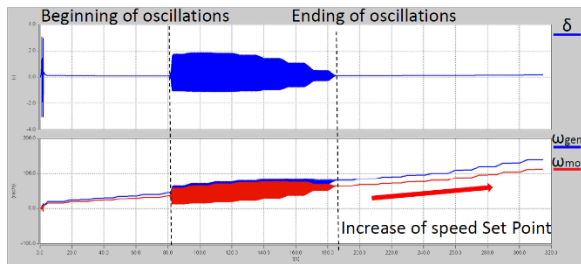


Figure 9 : Transient simulation of the system evolving between steady state stages in the same conditions as **Figure 8** with a speed set point increase

The idea is then to compare the root locus of the **Figure 8** with the transient simulations of **Figure 9** in order to see if whether or not the root locus matches with the transient simulations : that is to say, if the beginning and ending of oscillations coincide with the passing in the right-hand plane.

After the study of this approach, it appears that the root locus approach coincides under approximations of few radians per second with any transient simulations.

For example, on these figures, the oscillations coincide with the passing in the right-hand plane with an approximation of a few radians per second (comparison here on the motor mechanical speed), approximation mostly due to the “small signal linearization” that gives the root locus approach :

Transient simulation		Root locus	
Speed set point for the beginning of oscillations (rad/s)	Speed set point for the ending of oscillations (rad/s)	Speed set point for the beginning of oscillations (rad/s)	Speed set point for the ending of oscillations (rad/s)
32	64	31-32	64-65

Table 1 : Summary and comparison of the speed set point values of the **Figure 8** and the **Figure 9** for the characterization of the oscillations

Therefore, the root locus approach can be seen as a first visual stability criterion for this AC architecture as it enables to predict potential instabilities in the functioning of the AC architecture thanks to a root locus representation.

Conclusions

A complete state model has been established, enabling to fully describe a “power electronic-less” AC architecture, only composed of two PMSM directly linked through an AC bus. From that nonlinear state model, dynamic and steady state analysis are possible.

From this model, it has been analysed that oscillations and sometimes system stall may appear with this architecture, certainly because of the stiffness of this AC architecture. These situations are depending on the parameters of the AC architecture (both machines but also especially the controller parameters driving the gas turbine).

In order to describe these oscillations a stability analysis is derived thanks to a small signal linearization of the previous state model allowing to display the system root-locus. The complete study of this linearized approach allows to conclude that it is appropriate for a first characterization of the stability of this AC architecture.

Beyond that methodological aspect, one can conclude so far that stable operation range can be reached for this simple AC architecture, the stable operation being depending to the parametrization of the system. The future issue is then to prove that a safe and stable operation can be obtained by setting an appropriate sizing of both machines and also by adjusting the speed controller.

References

- 1 M. Pettes Duler, “Integrated optimal design of a hybrid-electric aircraft powertrain”, PHD Thesis of Toulouse University, April 23rd, 2021.
- 2 P. Kundur, Power System Stability and Control, Power System Engineering Series, 1994
- 3 M. Kostenko and L. Piotrovski, Electrical Machines : In two Volumes, MIR Publishers, 1969
- 4 N. Bernard, Machine Synchrone de la boucle ouverte à l'autopilotage, Revue 3EI, 2002, n°30, pp. 24-39
- 5 N.K. Borer, M.D. Patterson, J.K. Viken, M.D. Moore, S. Clarke, M.E. Redifer, R.J. Christie, A.M. Stoll, A. Dubois, J.B. Bevirt, A.R. Gibson, T.J.Foster, P.G.Osterkamp, Design and Performance of the NASA SCEPTOR Distributed Electric Propulsion Flight Demonstrator, AIAA, 2016
- 6 K.R. Antcliff and F.M. Capristan, Conceptual Design of the Parallel Electric-Gas Architecture with Synergistic Utilisation Scheme (PEGASUS) Concept, AIAA, 2016
- 7 X. Zhang, C.L. Bowman, T.C. O’Connell, K.S. Haran, Large electric machines for aircraft electric propulsion, IET journals, 2018
- 8 H. Ben Ahmed, N. Bernard, G; Feld, B. Multon, Machines synchrones en régime permanent, Techniques de l’ingénieur - d3522, 2007